Astron. Astrophys. 329, 1028–1034 (1998)

ASTRONOMY
AND
ASTROPHYSICS

HST - GHRS observations of CO and CI in the β-Pictoris circumstellar disk*

A. Jolly[1], J.B. McPhate[2], A. Lecavelier[3], A.M. Lagrange[4], J.L. Lemaire[1,5], P.D. Feldman[2], A. Vidal Madjar[3], R. Ferlet[3], D. Malmasson[1], and F. Rostas[1]

[1] DAMAP et URA 812 du CNRS, Observatoire de Paris-Meudon, F-92195 Meudon Cedex, France
[2] Department of Physics and Astronomy, Johns Hopkins University, Baltimore, Maryland 21218, USA
[3] Institut d'Astrophysique de Paris, CNRS, 98bis Bd Arago, F-75014 Paris, France
[4] Grouped'Astrophysique de Grenoble, CERMO BP53X, F-38041 Grenoble Cedex, France
[5] Université de Cergy-Pontoise, 33 Bd du Port, F-95011 Cergy-Pontoise, France

Received 1 April 1997 / Accepted 11 July 1997

Abstract. GHRS-EchA and G160M spectra of β-Pictoris have been obtained in the 1400-1600 Å range. A detailed analysis of the CO A-X (0-0, 1-0, 2-0) bands and of the CI λ1561 Å multiplet is presented. A column density of the order of 2 10^{15} cm^{-2} is found for both species. For CO, the rotational temperature is found close to 20 K and the turbulent Doppler width is b=0.8 km.s^{-1}. Including the ^{13}CO lines in the fit allows an estimate of the ^{13}CO abundance: R=^{12}CO/^{13}CO=20. This anomalous ratio is tentatively interpreted as being due to chemical fractionation. For the CI triplet, the absorption profile is best fitted by a combination of four velocity components matching those observed independently at the same moment from ground in the CaII H and K lines. The most intense component corresponds to zero relative velocity while the others are shifted by 3 to 10 km s^{-1}. The large turbulent width of the components (4.2 km s^{-1}), the statistical population of the ground state fine structure levels and the similar column densities of CI and CO are interpreted as indicating that CI is formed by photodissociation of CO and destroyed by photoionization. The velocity structure would then indicate that part of CI is formed at large distance ($\sim$100 AU) from CO evaporating from cometary bodies while another part originates closer to the star from fast moving cometary bodies with high excentricity.

Key words: stars: circumstellar matter – stars: β-Pictoris

1. Introduction

Since the discovery of a circumstellar disk of dust and gas around β-Pictoris, there has been growing evidence that comets are present around the star. Early spectroscopic observations of infalling gas at high velocities were attributed to star grazing and evaporating comets (Lagrange et al. 1987, Ferlet et al. 1987). Simulations based on this model reproduced quite well the first variable features observed (Beust et al. 1990, 1991) and the subsequent ones, recorded over more than ten years now (see for more details Ferlet and Vidal-Madjar, 1995; Lagrange et al. 1996a and Beust et al. 1996 and references therein).

Also, the IUE detections of over ionized infalling gas (Lagrange et al. 1989, Deleuil et al. 1993) were well explained by the evaporating infalling bodies scenario (Beust & Tagger 1993). GHRS observations of β-Pictoris (Boggess et al. 1991, Vidal-Madjar et al. 1994) brought strong additional support to this scenario: the size of the infalling cloud and the detailed shape of the variable features appeared to be matched by the simulations. Two very important discoveries were achieved with GHRS: the detection of CO and CI (Vidal-Madjar et al. 1994), whereas all attempts to detect molecular species such as CO, SiO, etc.. through their microwave emission have failed (Saldovini & Galletta, 1994, Liseau 1996). Since both species are short lived, CO being destroyed by photodissociation and CI by photoionization, they have to be permanently replenished in order to maintain an observable column density. It was proposed that evaporation of comets was responsible for the presence of CO, and that photodissociation of CO was in turn responsible for the presence of CI. Lecavelier et al. (1996) went even further and proposed that the evaporation of comets could also explain the distribution of small size dust particles in the disk. Other independent indications of the presence of comets were given by the observation of the 10 μm silicate feature (Knacke et al. 1993). This feature is due to small silicate grains, which are also short lived and should be permanently produced. The shape of the feature does not match that observed in any astrophysical medium except comets in our Solar System. Hence the 10 μm silicate feature also favors the hypothesis of active comets orbiting around the star. The first CO and CI observations were made

Send offprint requests to: F. Rostas

* Based on observations with the NASA/ESA Hubble Space Telescope, obtained at the Space Telescope Science Institute which is operated by the Association of Universities for Research in Astronomy Inc., under NASA Contract NAS5-26555.

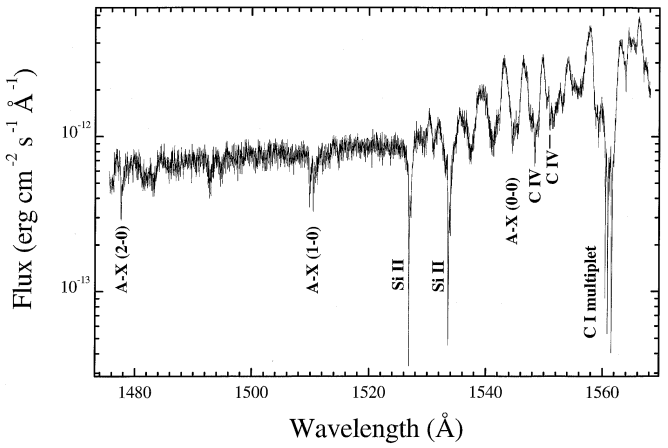

Fig. 1. Composite β-Pictoris spectrum obtained with the HST-GHRS instrument (G160M grating)

at medium resolution prior to the HST refurbishment. The 1994 refurbishment enabled higher resolution observations at short wavelengths. We thus reinvestigated the CO and CI spectral regions with the EchA and G160M gratings in order to further constrain the characteristics of these features. We present in Section 2 the observations. The results of the observations are given in section 3 and discussed in Sect. 4.

2. Observations

The GHRS observations presented here are part of a multiwavelength and multisite campaign on β-Pictoris that took place in Nov 1994. Many wavelength ranges were investigated. They are described and analysed in Lagrange et al. (1997). We focus in the present paper on the 1400 to 1600 Å domain, where the CO and CI features are observed. Table 1 gives the log of the observations and Fig. 1 a general view of the observed spectrum.

During the HST observations, a continuous monitoring of the variability of the CaII lines was pursued. The observations included many sites in the Southern Hemisphere. The resolving power ranged between a few 10^4 and 10^6 (see details in Lagrange et al. 1997). During the HST CO and CI observations, variable lines were observed in the CaII features, some of them at very low velocities (less than 10 km s^{-1}) with respect to the star velocity. When observed at high resolving power (10^5), the central absorption features appeared to be asymmetrical with an enhanced red wing. When observed at ultra high resolution (10^6), they appeared to be made of several components with velocities ranging between 17 and 32 km/s. The very low velocity lines may contribute to 50 % of the observed feature.

The data reduction performed is described in Vidal-Madjar et al. (1994). It basically recombines FP split sub exposures. However, the present observations, made in a wavelength range where the β-Pictoris flux is relatively low, did not allow the standard cross-correlation procedure to be performed on the Ech A spectra due to the relatively low S/N ratio of each individual sub-exposures of the FP-SPLIT GHRS pattern. It was thus necessary to rely on the standard wavelength calibration provided with each individual sub-exposure to coadd them and produce the final spectra presented here. The standard wavelength calibration being provided with an absolute precision of the order of $\pm$3 km/s, i.e. of the order of the Echelle-A linewidth, one would expect in such a process to degrade the nominal Echelle-A resolving power. It will be seen below that, indeed we have been led to consider that the effective resolving power of the Echelle A spectra is only of the order of 40.000 (instead of 60.000). This figure is compatible with the calibration uncertainty quoted above. For the G160M spectra on the contrary, the nominal resolution of 20.000 was achieved and all the spectra presented are based on the standard HST wavelength calibration.

3. Analysis of the spectra

3.1. CO A-X bands

The three observed bands of the CO $A^1\Pi$-$X^1\Sigma^+$ transition are strongly saturated, allowing weak features such as the ^{13}CO bands to be observed and strongly emphasizing a satellite of the (1-0) band. This satellite band is attributed to the F_3 component of the spin-forbiden transition $d^3\Delta$(v'=5) - $X^1\Delta^+$(v"=0) which borrows intensity through an interaction between the $d^3\Delta(5)$ and $A^1\Pi(1)$ levels. This transition was observed but not identified by Hanson et al. (1992) on IUE spectra. It was thoroughly analysed in the laboratory by Herzberg et al. (1970). The mixing coefficients were calculated by Le Floch et al. (1990). The resulting line positions and intensities have been tabulated recently by Morton and Noreau (1994). The A-X transition of ^{13}CO (0<v'<9) has been analysed recently by Haridass et al. (1994) thus allowing a complete simulation of the optically thin spectrum of the three bands.

The simulation is performed, as described by Jolly et al. (1997), using the perturbation model of Field (1971, 1972) and Le Floch (1987, 1989). Introducing a line profile, the normalized spectrum $S(\lambda)$ such that $\int S(\lambda)d\lambda$=1 is obtained. The intrinsic (or optically thin) calculated $\sigma(\lambda)$ spectrum is then $\sigma(\lambda)$=$\sigma_T S(\lambda)$ where σ_T is the band integrated absorption cross section with $\int \sigma(\lambda)d\lambda$=$\sigma_T$. As an illustration, the calculated optically thin $\sigma(\lambda)$ spectrum of the 1-0 band, including contributions of ^{12}CO, ^{13}CO and of the $d^3\Delta$-$X^1\Sigma^+$(5-0) transition of ^{12}CO, is displayed in Fig. 2.

The calculated optically thin cross section spectra $\sigma(\lambda)$ are then introduced in the Beer-Lambert expression and convolved with the instrument function according to:

$$I(\lambda) = \int I_0(\lambda')P(\lambda - \lambda')e^{-\sigma(\lambda')N}d\lambda' \quad (1)$$

where N is the column density of the absorbing molecules and P(λ) is the instrument profile which here, as in most cases, is considerably wider than the intrinsic Doppler profile of the lines. This difference introduces strong saturation effects when $\tau(\lambda)$ = $N\sigma(\lambda)$ is not much smaller than 1, which is the case here.

The analysis of the strongly saturated spectra requires a careful determination of the continuum background $I_0(\lambda)$. For the

Table 1. HST-GHRS Exposure log-table

Obs ID	grating	Spectral range (Å)	Date../../..	Hour (UT)	exposure time (s)
z2kb0107p	G160M	1476 – 1511	23/11/94	16:27	2000
z2kb0109p	G160M	1500 – 1535	23/11/94	17:52	2000
z2kb010bp	G160M	1533 – 1568	23/11/94	19:17	1200
z2kb010ep	echB	1543 – 1551	23/11/94	20:37	3000
z2kb010gp	echA	1559 – 1567	23/11/94	22:18	1200
z2kb010in	echA	1608 – 1616	23/11/94	22:45	1200
z2kb010kp	echA	1543 – 1551	23/11/94	23:54	2000
z2kb010lp	echA	1558 – 1567	24/11/94	00:30	1200
z2kb010mp	echA	1608 – 1616	24/11/94	01:38	1200

(1-0) and (2-0) bands we have used the continuum calculated by Kurucz (1991, 1992, 1996) after suitable renormalization for each band. It is seen in Fig. 3 that for these two bands the Kurucz continuum is adequate. Its long term fit to the details of the baseline gives confidence in its variation under the bands. For an unexplained reason, this is obviously not the case at the 0-0 band for which we have used a 6th degree polynomial to represent the continuum. Calculating $I(\lambda)/I_0(\lambda)$ produces the normalized absorption spectra which will be compared to the simulated ones.

The calculated absorption spectra are least squares fitted to the observed ones. They have first to be shifted in wavelength to account for the radial velocity of β-Pictoris. This shift is determined either by hand using the sharp band heads as a reference or as a parameter in the least squares fitting procedures. The shift is consistently found by both techniques as 120 mÅ i.e. 23 ± 1 km.s^{-1}. This is in accord with the heliocentric velocity of β-Pictoris (21 km.s^{-1}) considering the uncertainty in the calibration of the GHRS spectra (1 to 2 km.s^{-1}). The integrated absorption cross section σ_T is held fixed at the tabulated values (Eidelsberg et al., 1992). In general the free parameters in the fit are N, the column density of ^{12}CO, R the ^{12}CO/^{13}CO ratio, b the turbulent velocity which defines the intrinsic Doppler width of the lines and T, the rotational temperature. In some instances it was found useful to leave the instrument width, and/or the Doppler shift as additional free parameters.

3.2. The CI λ1561 Å multiplet

The multiplet comprises 6 lines forming three separate unresolved components originating from three fine structure sublevels of the ground state at respective energies of 0, 16.4 and 43.4 cm^{-1}. The wavelengths and oscillator strengths of the individual lines are given in Morton (1991). The synthetic absorption spectrum is calculated with the technique described above with the nominal instrument width (20 mÅ for EchA spectra and 66 mÅ for G160M). The continuum around 1561 Å was fitted with a constant and five broad gaussian absorption features. A small value ($\approx 0.5\ 10^{-13}$ erg.cm^{-3}.s^{-1} Å^{-1}) was subtracted from the spectra if needed to set at zero the bottom of the totally absorbed features of the multiplet. The calculated spectrum was least squares fitted to the observed one, leaving as free parameters the ground state excitation temperature T_G, the CI column density N_C, the turbulent velocity parameter b and the heliocentric velocity v.

It was found however that, although the general shape of the spectrum was accurately described in these fits, a dip in the absorption at 1561.45 Å was not accounted for (see Fig. 5). In a second step, multivelocity models were explored empirically and it was found that combinations of four or more components displaced by a few km s^{-1} could represent the 1561 Å component of the triplet including the dip. It was not found possible to determine all parameters by a least squares fitting procedure. However, as will be seen below, the component velocities could be fixed by reference to the independent observations of CaII lines made at the same time, and satisfactory fits were obtained.

4. Results

4.1. CO A-X bands

The best fitting calculated CO spectra are compared to the observed ones in Fig. 4. The fit was run simultaneously on the three low resolution bands, on the one hand, and independently on the high resolution 0-0 band. Studying first the high resolution 0-0 band it became clear that the Echelle-A spectra of the 0-0 band did not have the nominal resolution. This showed up on the trough between lines which does not return to zero as it should at the nominal resolution. The loss in resolution is most probably due to the fact that the low signal/noise ratio did not allow recombining the individual FP-SPLIT spectra by the cross correlation technique. The instrument width was left as a free parameter in the fit which resulted in an instrument width of 36 mÅ (resolving power: 40000). The other parameters obtained from the fit were:
N=3.7 10^{15}cm^{-2}, b=0.77 kms^{-1}, T=15.4 K, R=30

It was found however that the instrument width determined by the fit seemed too large and fits were run with fixed widths varying from 25 to 36 mÅ.

The parameters obtained varied in the range:
N=1.8-3.7 10^{15} cm^{-2}, b=0.76-0.83 km.s^{-1}, T=16.5-15.4 K, R=16-30.

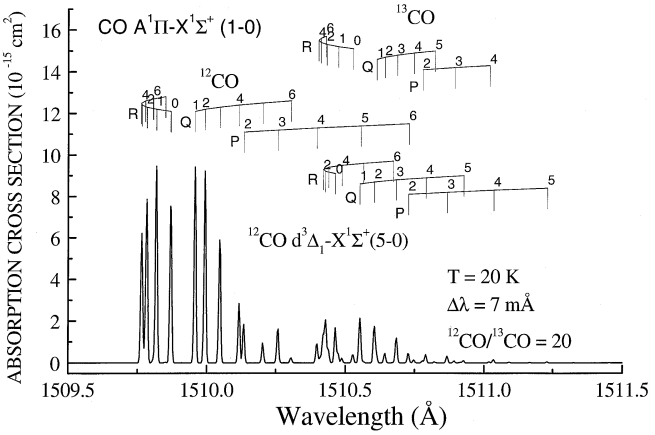

Fig. 2. Optically thin, calculated absorption spectrum of the CO $A^1\Pi$ - $X^1\Sigma^+$ (v'=1, v"=0) band. The parameters used correspond to those obtained by the fit shown in Fig. 4

When fitting simultaneously the three G160M spectra with the nominal resolving power of 20.000 one obtains:
N=1.39 10^{15} cm^{-2}, b=0.76 $km.s^{-1}$, T=22.7 K, R=17.
These results are close to those obtained from the high resolution 0-0 band with an instrument width of 25 mÅ.

Finally, the set of parameters found to conservatively represent the four CO absorption bands observed is displayed in Table 2. It is felt that this set of parameters which is compatible with the four available spectra constitutes a robust solution which fits very well all the important features of the data and that the most important results:

$$N \approx 2.10^{15},\ T \approx 20\ K \text{ and } R = {}^{12}CO/{}^{13}CO \approx 20$$

are well established. Indeed, it is clear that the high resolution (0-0) band definitely requires a temperature in the 15-20 K range. Also the $^{12}CO/^{13}CO$ ratio of about 20 is supported by three details in the spectra:

1. The band head at 1544.3 Å which is entirely due to ^{13}CO is very clear in the high resolution (0-0) band spectrum. It definitely appears on the low resolution spectrum also.
2. It is seen in Fig. 4 that the trough at 1544.55 Å in the high resolution 0-0 band would be significantly deeper without the ^{13}CO contribution.
3. The ^{13}CO contribution in the 2-0 band is completely separate from that due to ^{12}CO. Admittedly, due to the low signal to noise ratio it would not by itself be sufficient to determine the ^{13}CO abundance, but in conjunction with the other observations its reality seems definitely established.
4. The very surprising intensity of the $^3\Delta^{-1}\Sigma^+$ satellite in the 1-0 band is largely due to saturation effects, however the contribution of ^{13}CO is indispensable to reach a peak height slightly higher than the main ^{12}CO peak.

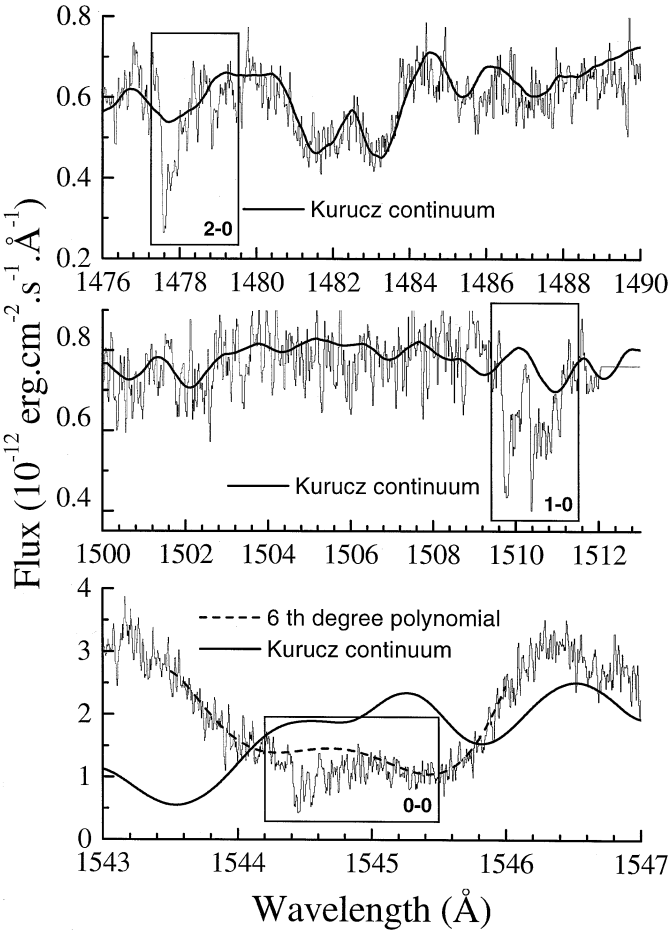

Fig. 3. Stellar continuum intensities used to calculate the absorption coefficients of the CO bands. For the 1-0 and 2-0 bands the absolute intensities calculated by Kurucz were normalized to fit the observations. In the region of the 0-0 band the Kurucz continuum was replaced by a 6th degree polynomial fit.

4.2. The CI λ1561 Å multiplet

4.2.1. Single velocity fit

The best fitting values found for the free parameters in the single velocity model are shown in Table 2. The calculated and observed spectra are compared in Fig. 5. As noted above, the absorption dip at 1561.45 Å cannot be reproduced. The CI column density is found very similar to that of CO while the turbulent velocity is much higher. The very high excitation temperature of the ground state indicates that the three substates are statistically populated. These facts are interpreted below as indicating that CI is formed by the photodissociation of CO.

4.2.2. Multivelocity fit

The empirical 4-component multivelocity fits which were found to reproduce satisfactorily the 1561.5 Å component of the triplet produced a set of velocities which turned out to be very close to those obtained in the very high resolution (10^6) ground based observations of the central component of the CaII H and K lines

Table 2. Results from spectral fitting

	System velocity ($km.s^{-1}$)	Column density N(cm^{-2})	Turbulent width b ($km.s^{-1}$)	Temperature T (K)	$^{12}CO/^{13}CO$ R
CO	23 ± 3	(2 ± 1) (15)	0.8 ± 0.05	20 ± 5	20 ± 5
CI Single velocity model	22.4	1.4 (15)	7.3	>100	_
Ca II (K)	17.7	2.2 (12)	3.0	_	_
From UHRF	20.8	6.3 (12)	0.7	_	_
(Lagrange et al. 1997)	23.5	1.4 (12)	3.5	_	_
	31.0	0.8 (12)	3.5	_	_
CI	17.9	3.9 (14)	4.2	>100	_
Four velocity	21	1.0 (15)	4.2	>100	_
model	23.7	2.2 (14)	4.2	>100	_
	31.2	1.3 (15)	4.2	>100	_

made on UHRF very close in time to the present data (Lagrange et al. 1997). This suggested that part of the CI observed could be formed, not in the stable region where CO is observed at zero relative velocity shift, but closer to the star where refractory elements are evaporated from infalling comet-like bodies. Following this lead, four-component CI profiles were calculated using relative velocities and intensities matching those of the CaII lines. The CI calculated profile was fitted to the observed one by adjusting the total column density, and the b value (assumed to be the same for all components). The populations of the ground state fine structure levels were taken to be equal and the whole profile was slightly velocity shifted, as necessary for the fit. The profiles obtained fit rather well the observed one (Fig. 5). The parameters used for the fit are listed in Table 2. It is seen that the four component velocities are equal to those of CaII within the calibration errors. The b value however is significantly larger for CI.

5. Discussion

5.1. CO

The present results confirm the previous detections of CO and CI in the stable gas surrounding β Pictoris (Deleuil et al. 1993; Vidal Madjar et al. 1994). For CO, the simultaneous analysis of the A-X (0-0), (1-0) and (2-0) absorption bands allows a reliable determination of the column density and turbulent width. The CO column density tentitavely determined in Vidal-Madjar et al. (1994) is confirmed. Furthermore, ^{13}CO has been detected for the first time and its abundance can be determined with reasonable security because it appears in the three bands with different shifts.

These results tend to confirm the models which attribute the origin of CO and the dust in the β-Pictoris disk to the evaporation of kilometer size cometary type bodies at relatively large distances from the star (A. Lecavellier et al. 1996).

1. The CO volume density and the total CO mass deduced from the column density measured are respectively of the order of N_{CO}=1 cm^{-3} and $M_{CO} \approx 5.10^{20}$kg assuming the disk has the shape of a wedged torus of average radius r_0=100 AU subtending an angle of 10°.
2. If one assumes typical solar system cometary mass abundance ratios i.e.: Ψ_{CO}=CO/gas≈ 0.1 and Ψ_{gas}=gas/dust≈10. If φ=0.1 is the proportion of the dust evaporated from the comets remaining in the disk and if the lifetimes of CO and the dust are respectively 10^3 and 10^6 years, one obtains a total dust mass.
$M_d = M_{CO} . \varphi . \Psi_{CO}^{-1} . \Psi_{gas}^{-1} . t_d / t_{CO} = 10^2 M_{CO} = 5\ 10^{22}$kg.
This value is close to the value independently determined for the total dust mass by submillimeter observations (Zuckerman & Becklin 1993).
3. The 20 K rotational temperature found for CO is close to the 25 K estimated sublimation temperature of CO at comet surfaces (A. Lecavelier 1996).

The high ^{13}CO abundance found in this study can be accounted for by chemical fractionation through the reaction.

$^{13}C^+ + {}^{12}CO \rightleftharpoons {}^{13}CO + {}^{12}C^+ + 35$ K

This process which favours ^{13}CO at temperatures below 35 K, is expected to predominate over the radiative fractionation, which in molecular clouds selectively photodissociates ^{13}CO, because here the small transverse dimensions of the disk will not allow ^{12}CO to self shield so that ^{12}CO and ^{13}CO are both photodissociated at the same rate. Assuming chemical equilibrium at 20K one obtains (Sheffer et al. 1992):
$R = {}^{12}CO/{}^{13}CO = \exp(-35/T)\ {}^{12}C/{}^{13}C = 0.17\ {}^{12}C/{}^{13}C$.
So that at 20 K, $R = {}^{12}CO/{}^{13}CO = 20$ implies that $^{12}C/^{13}C = 117$.
Conversely if the $^{12}C/^{13}C$ ratio is fixed at the standard value of 70 the temperature compatible with the fractionation equilibrium is 28 K. Considering the uncertainties in the experimental values of R and T, this indicates that the abnormaly high ^{13}CO abundance found can be explained by chemical fractionation without resorting to an abnormal $^{12}C/^{13}C$ ratio. Assuming equilibrium for the chemical fractionation process is quite reasonable. Indeed, the rate constant for the forward reaction has been measured at 80 K by Smith and Adams (1980): $K_f = 6.8\ 10^{-10}$ $cm^3.s^{-1}$. The ^{12}CO density is of the order of 1 cm^{-3} so that the reaction rate of $^{13}C^+$ is of the order of 10^{-9} s^{-1}, one order of magnitude larger than the photodissociation rate of CO in the

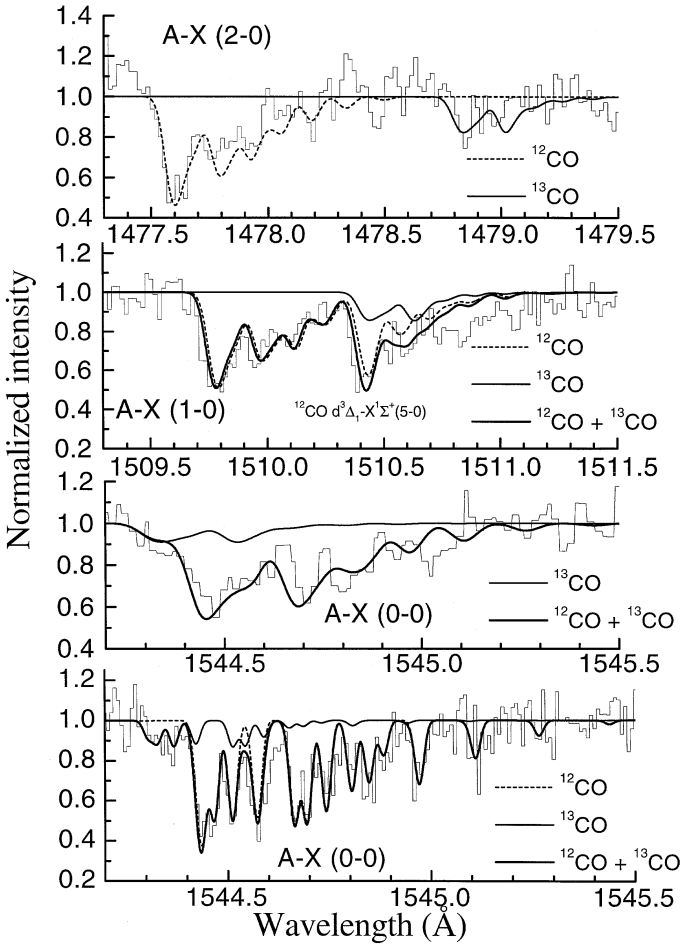

Fig. 4. Observed and best fitting calculated spectra of the (2-0), (1-0) and (0-0) CO A-X absorption bands. The first three panels are G 160 M spectra (resolution 20.000). The lower panel is an Ech-A spectrum (effective resolution 40.000, see text). The three low resolution spectra were fitted simultaneously with a single set of parameters. Note on the 2-0 band the feature at 1510.4 Å which is a superposition of a strong (16%) forbidden transition $d^3\Delta$-$X^1\Sigma^+$ (5-0) and the contribution of ^{13}CO. Due to the strong saturation this combination reaches a peak intensity slightly larger than the main band. Note on the high resolution 0-0 band the contribution of ^{13}CO which appears clearly at the band head and in the trough at 1544.55 Å. The Ech-A spectrum was fitted after fixing the instrument width at 25 mÅ (R=60.000).

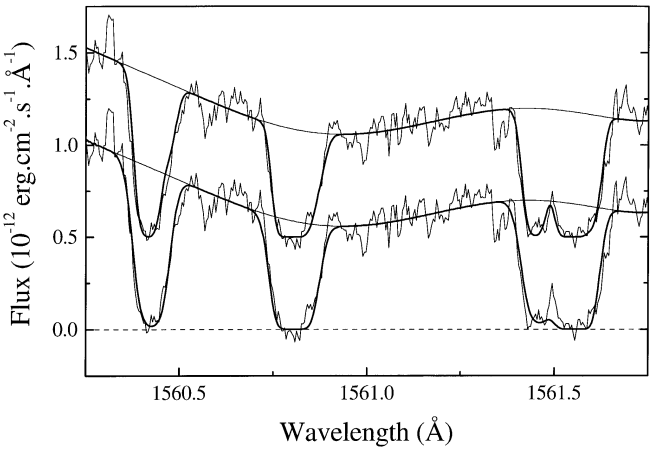

Fig. 5. Ech-A spectrum of the CI λ1561 Å triplet. (*Lower trace*: fitting with single velocity model spectrum; *Upper trace*: fitting with a 4-velocity model spectrum. The trace is displaced upwards by 0.5 10^{-12} flux units for clarity).

interstellar radiation field i.e. 2 10^{-10} s^{-1} (Van Dishoeck and Black 1988) meaning that the fractionation reaction can reach equilibrium during the lifetime of CO, which is determined by its photodissociation rate.

5.2. CI

The relative CO to CI abundances and the widths of the zero velocity CI absorption are well explained if one assumes that CI in the stable gas is predominantly formed by photodissociation of CO and destroyed by photoionization. Indeed, in the interstellar radiation field, the CO photodissociation rate is evaluated at 2 10^{-10} s^{-1} (Van Dishoeck and Black 1988) while the CI ionization rate would be 1.4 10^{-10} s^{-1} (Lang 1980). At equilibrium this leads to similar CO and CI volume densities as observed. The photodissociation threshold of CO is at 11.1 eV, Huebner et al. (1992) calculated that the (average) excess energy above this threshold in the solar EUV radiation field is 2.57 eV, which corresponds to a velocity of about 5 km s^{-1} for the CI atoms formed by photodissociation. Therefore the Doppler width of about 4 km s^{-1} found for the component lines can reasonably be interpreted as due to the kinetic energy of the C atoms formed by photodissociation of CO. The statistical population distribution of the ground level spin substates of CI is also expected from a photodissociation process with a relatively high excess energy of the exciting photons.

The velocity structure of the CI absorption lines seems to indicate that a part of the CI observed does not belong to the same stable zero velocity gas layer as CO. That part could be produced nearer to the star, together with the refractory species such as Ca, by evaporation of comets having strongly elliptical trajectories. The b values observed are somewhat larger for the shifted components of CI than for CaII. This could indicate that CI is formed in this region also by photodissociation of CO which would be the parent molecule initially evaporated by the infalling comets. However the interpretation of the shifted components is far from straightforward, it should in particular take into account the dynamics of the released gas including radiation pressure and ejection velocity. However a part of the stable CI component could also be formed near the star.

6. Conclusion

A careful analysis of HST-GHRS spectra of β-Pictoris allows the characterization of CO and CI in the stable gas component of the disk. The ^{13}CO isotopomer has been detected and its abundance could be determined in spite of an unfavourable signal to noise ratio and thanks to the simultaneous analysis of three separate absorption bands. The high ^{13}CO relative abundance

found ($^{12}CO/^{13}CO \approx 20$) is interpreted as the result of chemical fractionation.

The similar column densities determined for CI and CO, the large Doppler width of the CI lines and the statistical population distribution of the CI ground state sublevels indicate that CI must be formed predominantly by photodissociation of CO. The CO column density of $\approx 2\ 10^{15}$ cm^{-2} and the CO rotational temperature of 20 K are both compatible with the disk formation models which rest upon the evaporation of cometary type bodies at large distances ($\sim$ 100 AU) from the star.

The analysis of the CI triplet in terms of four velocity components resembling those observed (nearly simultaneously) for CaII seems to indicate that part of the CI observed is not located at $\sim$ 100 AU in the zero velocity stable gas envelope where CO is observed. Rather it would be formed nearer to the star ($\sim$ 10 AU) where rapidly moving comets with high eccentricity evaporate and produce the velocity shifted variable spectral features of refractory elements. Part of the stable CI component could also be located in this region.

Acknowledgements. Thanks are due to R. KURUCZ for calculating the β-Pictoris continuum using the latest version of his codes.

The work of the Meudon group was partially supported by the "Programme Physique et Chimie du Milieu Interstellaire du CNRS".

Support for this work at Johns Hopkins University was provided by grant number G0-05406.02-93A from the Space Telescope Science Institute.

References

Beust H., Lagrange-Henri A.M., Vidal-Madjar A., Ferlet R., 1990, A&A, 223, 304

Beust H., Vidal-Madjar A., Ferlet R., Lagrange-Henri A.M., 1991a, A&A 241, 488

Beust H., Vidal-Madjar A., Ferlet R., Lagrange-Henri A.M., 1991b, A&A 247, 505

Beust H., Tagger M., 1993, Icarus 106, 42

Beust H., Lagrange A.M., Plazy F., Mouillet D., 1996, A&A 310, 181

Boggess A., Bruhweiler F.C., Grady C.A., Ebbets D.C., Kondo Y., Trafton L.M., Brandt J.C., Heap S.R., 1991, Ap. J. 377, L49

Deleuil M., Gry C., Lagrange-Henri A.M., Vidal-Madjar A., Beust H., Ferlet R., Moos H.W., Livengood T.A., Ziskin D., Feldman P.D., Mc Grath M.A., 1993, A&A 267, 187

Eidelsberg M., Rostas F., Breton J., Thieblemont B., 1992, J. Chem. Phys. 96, 5585

Ferlet R., Hobbs L.M., Vidal-Madjar A., 1987, A&A 185, 267

Ferlet R., Vidal-Madjar A., 1995, in Circumstellar Dust Disk and Planet Formation (10th IAP meeting), Editions Frontires

Field R.W., 1971, Thesis Harvard University

Field R.W., Wicke B.G., Simmons J.D., Tilford S.G., 1972, J. Mol. Spectr. 44, 383

Hanson M.M., Snow P., Black J.H., 1992, ApJ 392, 571

Haridass C., Huber K.P., 1994, ApJ 420, 433

Herzberg G., Hugo T.J., Tilford S.G., Simmons J.D., 1970, Can. J. Phys. 44, 3004

Huebner et al., 1992

Jolly A., Lemaire J.L., Belle-Oudry D., Edwards S., Malmasson D., Vient A., Rostas F., 1997, J. Phys. B. submitted

Knacke R.F., Fajardo-Acosta S.B., Telseco C.M., Hackwell J.A., Lynch D.K., Russel R.W., 1993, Ap. J. 418, 440

Kurucz R.L., 1991, In Crivellari L., Hubeny I., Hummer D.G. (eds) Stellar Atmospheres, Beyond Classical Models, Kluwer, Dordrecht, p. 441

Kurucz R.L., 1992, In Proc IAU Symposium 149, The Stellar Population of Galaxies, Barbuy B. and Renzini A. (eds) Kluwer, Dordrecht, p.225

Kurucz R.L., 1996, Private communication

Lagrange A.M., Ferlet R., Vidal-Madjar A., 1987, A&A 173, 289

Lagrange-Henri A.M., Beust H., Vidal-Madjar A., Ferlet R., 1989, A&A 215, L5

Lagrange A.M., Plazy F., Beust H., Mouillet D., Deleuil M., Ferlet R., Spyromilio J., Vidal-Madjar A., Tobin W., Hearnshaw J.B., Clark M., Thomas K.W., 1996a, A&A 310, 547

Lagrange A.M., Plazy F., Beust H., Mouillet D., Deleuil M., Ferlet R., Spyromilio J., Vidal-Madjar A., Tobin W., Hearnshaw J.B., Clark M., Thomas K.W., 1996b, A&A submitted

Lang K.R., 1980, Astrophysical Formulae, Springer, Berlin

Lecavelier des Etangs A., Vidal-Madjar A., Ferlet R., 1996, A&A 307, 542

Lecavelier des Etangs A., 1996, Thesis Université Paris VII, p.108

Le Floch A., Rostas J., Rostas F., 1990, Chem. Phys. 142, 261

Le Floch A., 1989, Thesis Université de Paris-Sud

Le Floch A., Launay F., Rostas J., Field R.W., Brown C.M., Yoshino K., 1987, J. Mol. Spectr. 121, 337

Liseau R. and Artymowicz P., 1996, A & A submitted

Morton D.C., Noreau L., 1992, ApJS 95, 301

Scheffer Y., Federman S.R., Lambert D.L., Cardelli J.A., 1992, ApJ 397, 482

Saldovini M. and Galletta G., 1994, A&A 285, 467

Van Dishoeck E.F., Black J.H., 1988, ApJ 334, 771

Vidal-Madjar A., Lagrange-Henri A.M., Feldman P.D., Beust H., Lissauer J.J., Deleuil M., Ferlet R., Gry C., Hobbs L.M., McGrath M.A., McPhate J.B., Moos H.W., 1994, A&A 290, 245

Zuckerman B., Becklin E.E., 1993, ApJ 414, 793

This article was processed by the author using Springer-Verlag LaTeX A&A style file *L-AA* version 3.